Parathyroid Imaging

Malak Itani, MD*, William D. Middleton, MD

KEYWORDS

• Parathyroid • Imaging • Radiology • Hyperparathyroidism • Ultrasound • Sestamibi
• Four-dimensional CT

KEY POINTS

- In patients with primary hyperparathyroidism, imaging of parathyroid glands plays an important role in localization of parathyroid adenomas prior to minimally invasive parathyroid resection.
- PHPT is caused by a single adenoma in 80% of cases, double adenomas in 5%, and multigland hyperplasia in 15%.
- Ultrasound and sestamibi scans are first-line imaging modalities with sensitivities of 80% and 84%, respectively.
- 4DCT is particularly valuable in cases of nondiagnostic or discordant ultrasound and sestamibi, or after failed neck operation.

INTRODUCTION

Primary hyperparathyroidism (PHPT) is an endocrine disorder defined by an elevated or inappropriately normal parathyroid hormone (PTH) level. Secondary hyperparathyroidism is elevated PTH in response to a metabolic alteration in patients with chronic kidney disease, typically due to high blood phosphorus levels, low levels of active vitamin D, or low blood calcium levels. With chronic elevation in PTH levels, true autonomy of the parathyroid glands occurs, leading to tertiary hyperparathyroidism. The role of imaging in hyperparathyroidism is to guide minimally invasive surgical interventions for PHPT.[1] Medical therapy remains the mainstay of management in secondary and tertiary hyperparathyroidism; therefore, the focus of this review is related to PHPT.

The prevalence of PHPT is 1 to 7 cases per 1000 individuals, with higher incidence among female and Black individuals, and the older population.[2] The highest prevalence of PHPT is among postmenopausal women and is estimated to be as high as 3%.[3] Sporadic PHPT is associated with exposure to ionizing radiation in childhood and with chronic lithium use.[4] The clinical presentation is usually nonspecific, and classically summarized as "stones, bones, groans, and moans" in reference to kidney stones, bone pain, abdominal groans from gastrointestinal symptoms, and psychiatric moans from central nervous system effects. Although this remains the clinical presentation in developing countries, the most common presentation in the United States and Europe is incidental asymptomatic hypercalcemia on routine laboratory analysis.[5] Normocalcemic hyperparathyroidism is a variant of PHPT recognized in 2009, usually diagnosed during investigations for low bone mineral density.[6] PHPT is caused by a single enlarged adenoma in 80% of cases, double adenomas in 5% to 10% of cases, multigland hyperplasia in 10% to 15% of cases (usually in familial endocrinopathies), and parathyroid carcinoma in less than 1% of cases.[1]

The parathyroid glands develop from the pharyngeal pouches in the fifth and sixth weeks of gestation and migrate caudally. The superior glands descend only a short distance, and thus their final location is less variable. They are typically located posterior to the thyroid, between the junction of the upper and middle thirds of the thyroid gland, and close to the inferior margin of the cricoid cartilage. The inferior glands migrate for a longer distance, more medially and inferiorly,

Mallinckrodt Institute of Radiology, Washington University in St. Louis School of Medicine, 510 South Kingshighway Boulevard, Campus Box 8131, St Louis, MO 63110, USA
* Corresponding author.
E-mail address: mitani@wustl.edu

Radiol Clin N Am 58 (2020) 1071–1083
https://doi.org/10.1016/j.rcl.2020.07.006

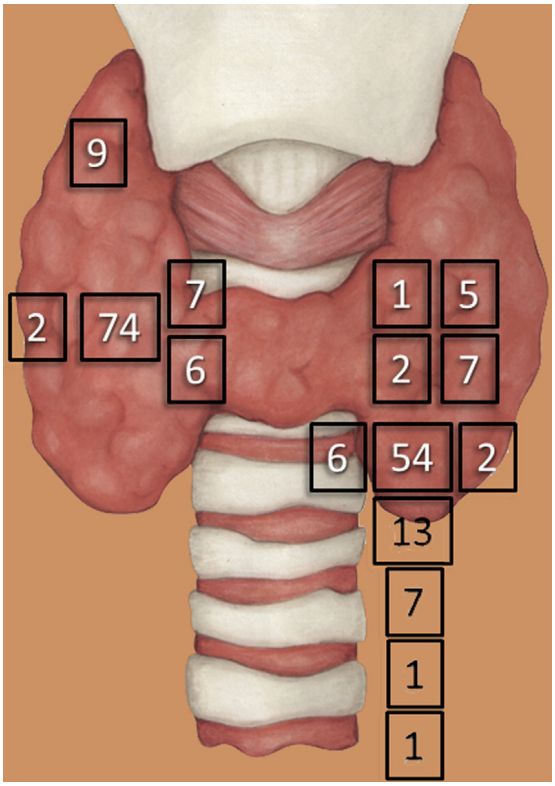

Fig. 1. Normal location of superior (patient right) and inferior (patient left) parathyroid glands. Previously published materials unchanged from the source. (*From* Mellnick VM, Middleton WD, Parathyroid Sonography. *Ultrasound Clinics* 2014; 9:339-350; with permission.)

and are thus more variable in location, and can be found anywhere from the angle of the mandible to the superior pericardium[7,8] (**Fig. 1**). Their classic location is directly posterior to the inferior margin of the thyroid gland (50% of cases) or 1 cm below it (15% of cases).[9] Ectopic locations for either superior or inferior glands include the tracheoesophageal groove, retroesophageal space, and rarely within the thyroid. Additional locations for ectopic superior parathyroid glands include retropharyngeal locations and posterior mediastinum, whereas ectopic inferior glands also can be found within the thymic capsule (38% of ectopic glands), carotid sheath, submandibular region, and down into the mediastinum.[1,10] Normal glands are very small in size, measuring 5 × 3 × 1 mm with estimated weight of 15 to 45 mg,[11] and are usually not visualized on imaging.[12] Most people have 4 parathyroid glands, although 2.5% to 15.0% have supernumerary glands[7] that can be located adjacent to the normal parathyroid glands or in the mediastinum and thymic capsule.[1]

IMAGING PROTOCOLS

Imaging modalities used for localizing parathyroid adenomas include ultrasound, 4-dimensional computed tomography (4DCT) and nuclear medicine scintigraphy. Imaging protocols are summarized in **Table 1**.

Ultrasound provides the advantages of being relatively inexpensive, using nonionizing radiation, delivering superb image quality in thin patients,

Table 1
Optimized imaging protocols for parathyroid adenoma detection

Protocol parameter	Ultrasound	4DCT	Scintigraphy
Scan range	Hyoid bone to thoracic inlet	Angle of mandible to carina	Parotid glands to lower heart
Patient positioning	Supine with neck hyperextension	Supine	Supine
Contrast or radiopharmaceutical	–	100 mL Omnipaque 350 at 5–6 mL/s	20 mCi Tc-99m sestamibi
Timing	–	Noncontrast Arterial phase (25 s) Venous phase (82 s)	Immediate at 5 min; delayed at 2 h
Acquisition	Linear high-frequency transducer	Slice thickness 0.75 mm	Immediate planar Delayed planar and SPECT/CT
Reconstruction	–	Axial, coronal, and sagittal 2-mm soft tissue windows	Axial, coronal, and sagittal typically at acquired thickness

Abbreviations: 4DCT, 4-dimensional CT; CT, computed tomography; SPECT, single-photon emission CT.

Table 2
Typical imaging features of parathyroid adenomas

Ultrasound	Solid well-circumscribed homogeneously hypoechoic ovoid structure Craniocaudal orientation of the long axis Variable internal vascularity
Scintigraphy	Persistent radiopharmaceutical retention on delayed images Extrathyroidal radiotracer uptake on SPECT images Tracer-avid soft tissue nodule on fused SPECT/CT images
4DCT	Early arterial enhancement Early washout on venous-phase images

Abbreviations: 4DCT, 4-dimensional CT; CT, computed tomography; SPECT, single-photon emission CT.

having a low carbon footprint, and especially providing concomitant evaluation of the thyroid gland. Its primary disadvantages are poor image quality in obese patients and operator dependency. It is typically performed after placing a pillow under the patient's shoulders so that there is hyperextension of the neck. A high-frequency linear transducer is used to allow for higher resolution. Additional evaluation of the superior mediastinum can be attempted with a high-frequency curved array transducer, such as the ones used for neonatal head or transvaginal ultrasound. Color Doppler or power Doppler can also help in the diagnosis. The examination initially focuses on the region posterior and inferior to the thyroid gland. Visualization of the paratracheal and paraesophageal regions is improved by turning the patient's head to the contralateral side and scanning from a lateral approach. When an enlarged parathyroid gland is not detected in the typical locations, survey of potentially ectopic locations also should be performed.[13,14]

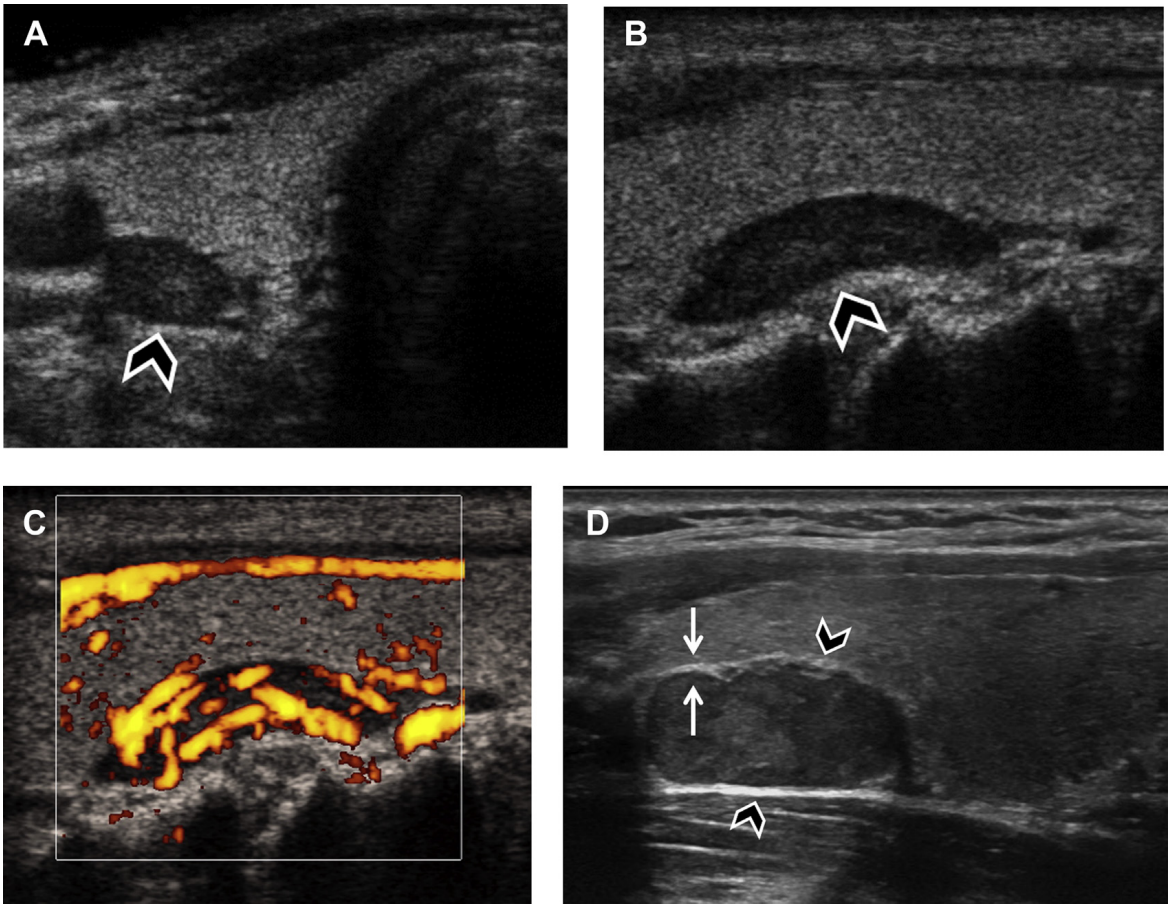

Fig. 2. Typical appearance of superior parathyroid adenoma. Transverse (*A*) and sagittal (*B*, *C*) views show the typical grayscale and power Doppler appearance of a superior parathyroid adenoma (*arrowheads*). It is a solid, ovoid, well-defined, hypoechoic nodule immediately posterior to the thyroid gland with increased internal vascularity. (*D*) Sagittal view in a different patient shows another superior parathyroid adenoma (*arrowheads*). The white line (*arrows*) that separates the parathyroid adenoma from the thyroid helps distinguish this nodule from a thyroid nodule.

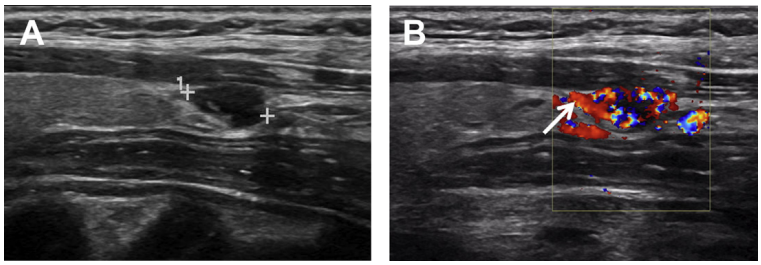

Fig. 3. Typical appearance of inferior parathyroid adenoma. Sagittal views show the typical grayscale (*A*) and color Doppler (*B*) appearance of an inferior parathyroid adenoma (*cursors* in *A*). It is a solid, ovoid, well-defined, hypoechoic nodule immediately inferior to the thyroid gland with increased internal vascularity and a polar vessel (*arrow* in *B*) exiting the superior border of the nodule.

Nuclear scintigraphy for parathyroid adenoma localization is usually performed with a single radiotracer (Tc-99m sestamibi). Immediate and 2-hour delayed planar images are obtained, in addition to an immediate or a delayed single-photon emission computed tomography (SPECT) or SPECT/CT acquisition. Because the most common cause for a false positive diagnosis of parathyroid adenoma on scintigraphy is a thyroid adenoma, a dual tracer subtraction technique can provide a way to characterize the latter. In the dual tracer technique, an additional imaging acquisition is performed with a thyroid imaging agent, such as Tc-99m pertechnetate or I-123, then subtracted from the sestamibi images.

4DCT is another major technique for localizing parathyroid adenomas. It was introduced as a multiphase CT with 4 phases (noncontrast, arterial, venous, and delayed), thus referred to as 4D, the fourth dimension being time. The fourth delayed phase is no longer considered necessary because the 3-phase protocol provides a good balance between radiation exposure and diagnostic performance.[15]

IMAGING FINDINGS/PATHOLOGY

Diagnostic Criteria

The diagnostic criteria for parathyroid adenomas are listed in **Table 2**. On ultrasound, the typical

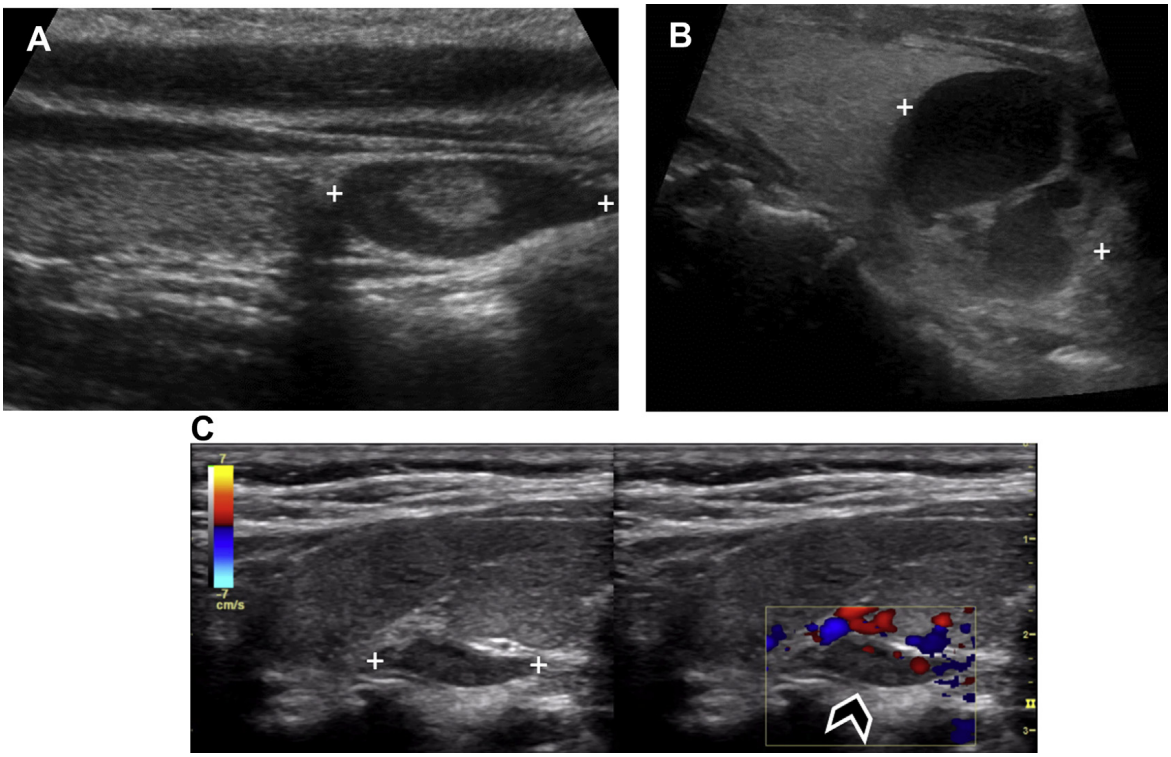

Fig. 4. Examples of atypical sonographic appearance of parathyroid adenomas (*cursors*) in different patients containing (*A*) internal echogenic components, (*B*) cystic spaces, and (*C*) minimal detectable internal flow (*arrowhead*), as seen on side-by-side grayscale and color Doppler images.

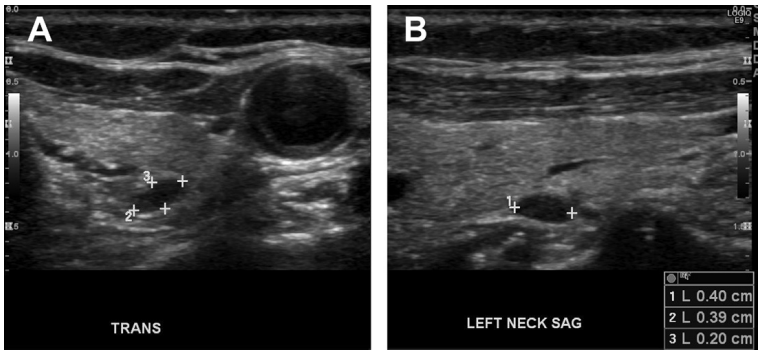

Fig. 5. Advantage of ultrasound in patients with thin neck. Transverse (*A*) and sagittal (*B*) grayscale images show a small superior parathyroid adenoma (*cursors*).

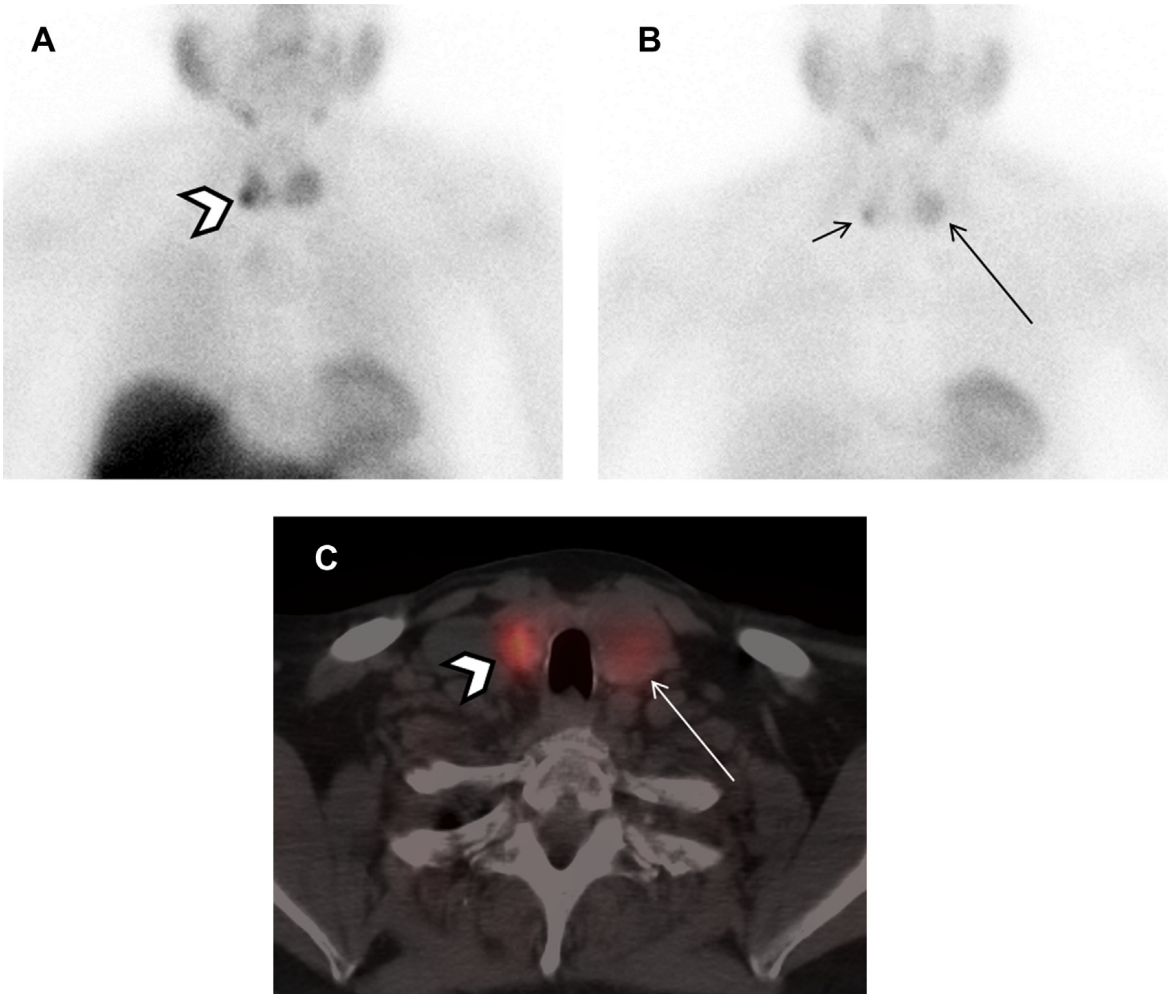

Fig. 6. Parathyroid adenoma on sestamibi scan. (*A*) Immediate and (*B*) delayed anterior images of Tc-99m sestamibi demonstrate a focus of intense uptake inferior to the right thyroid lobe (*arrowhead*) that becomes more conspicuous on the delayed 2-hour images (*short arrow*). Round area of focal uptake in the left thyroid on delayed images was confirmed histologically to be benign nodular hyperplasia (*long arrow*). (*C*) Axial fused SPECT/CT images localize the area of increased uptake to a small soft tissue nodule consistent with parathyroid adenoma. Again noted is the left thyroid lesion.

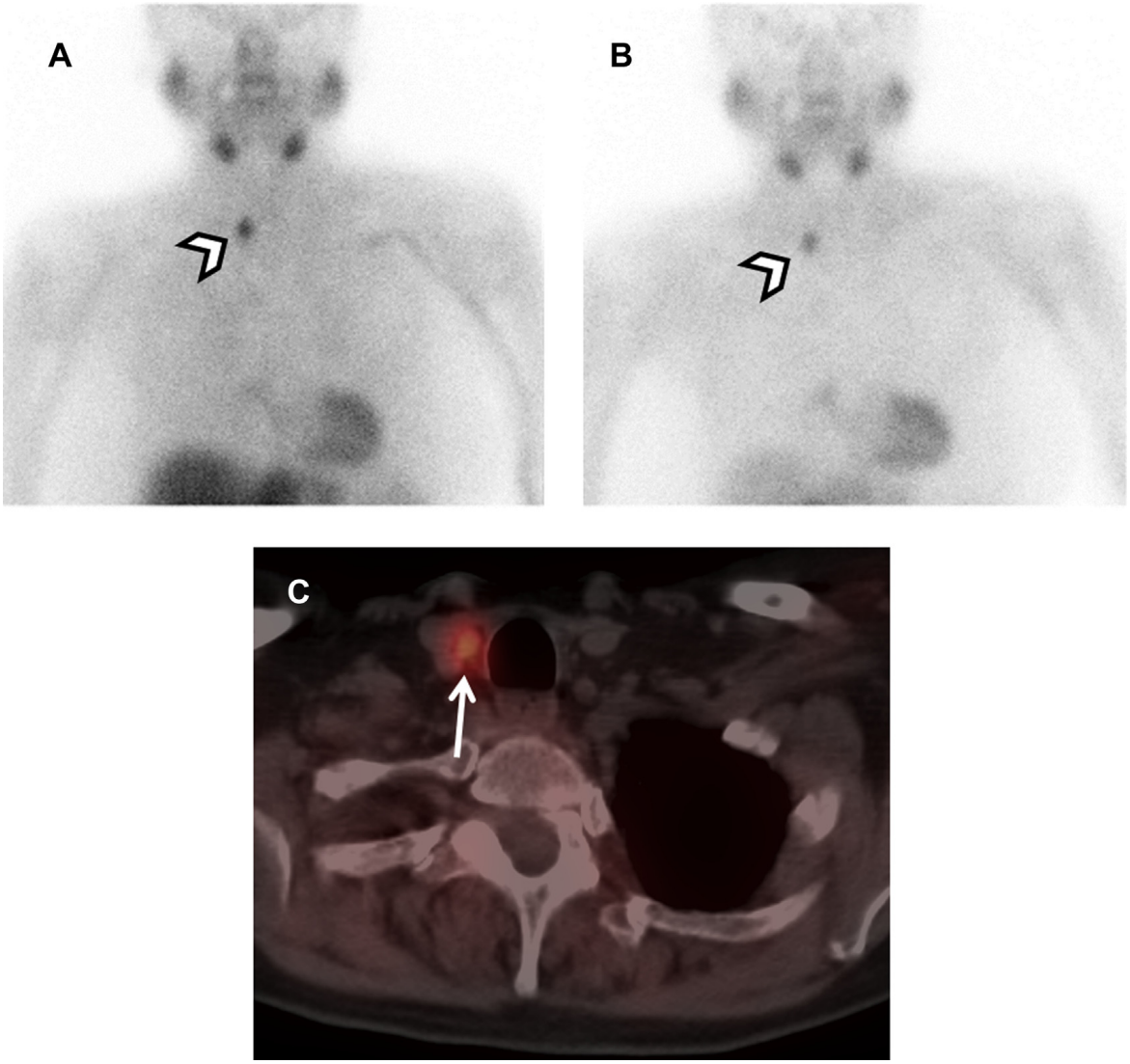

Fig. 7. Parathyroid adenoma on sestamibi scan. (*A*) Immediate and (*B*) delayed anterior images of Tc-99m sestamibi in a 73-year-old woman with prior thyroidectomy. A focus of increased uptake (*arrowheads*) in the right inferior neck is very clearly visualized given lack of uptake in the thyroid bed. (*C*) Fused axial SPECT/CT images localize the area of increased uptake to a small soft tissue nodule, consistent with parathyroid adenoma (*arrow*).

appearance for an enlarged parathyroid is a solid, well-circumscribed homogeneously hypoechoic ovoid structure, with its long axis oriented craniocaudally (**Figs. 2** and **3**). Less commonly, parathyroid adenomas can be isoechoic to the thyroid, contain focal hyperechoic areas, demonstrate internal heterogeneity, or contain cystic spaces (**Fig. 4**). Adenomas usually have detectable internal vascularity that may be less than, equal to, or greater than thyroid vascularity. However, when adenomas are small and deep, there may be no detectable flow. In some cases, there is a dominant peripheral vessel inserting or exiting at its pole. A large size of more than 3 cm, lobulated or irregular margins, extensive heterogeneity, or calcifications should raise concern for parathyroid carcinoma, particularly when the patient has more severe symptoms and laboratory abnormalities. The sensitivity of ultrasound for detecting parathyroid adenomas has been reported to range between 65% and 97%, with one meta-analysis concluding an overall sensitivity of 80%.[16] In another meta-analysis, ultrasound had a pooled sensitivity of 76.1% and positive predictive value (PPV) of 93.2% for detecting parathyroid adenomas.[15] Sensitivity for detection of small parathyroid adenomas is particularly good in patients with thin necks (**Fig. 5**). Sensitivity, however, decreases in obese patients, with multigland disease, after prior neck surgeries, and in the presence of

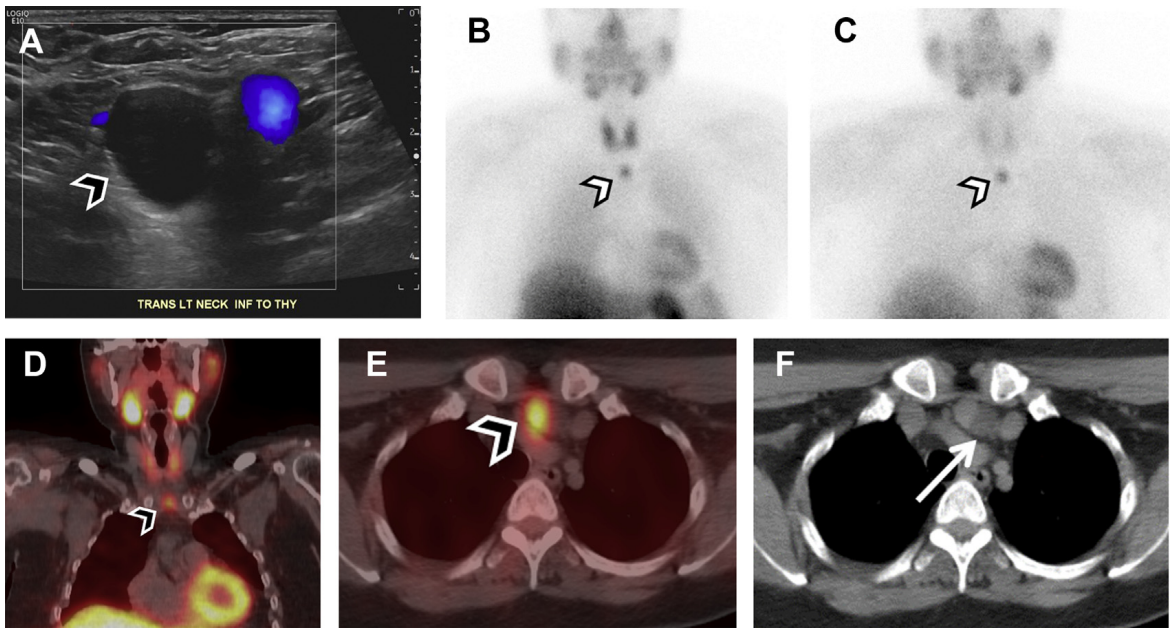

Fig. 8. Ectopic parathyroid adenoma on sestamibi scan. (*A*) Neck ultrasound identified a cyst (*arrowhead*) inferior to the left thyroid lobe. Sestamibi scan confirmed radiotracer uptake in the superior mediastinum on (*B*) immediate images, with persistent uptake on (*C*) 2-hour delay images (*arrowheads*). Findings were confirmed on SPECT/CT as seen on fused (*D*) coronal and (*E*) axial images (*arrowheads*), and on (*F*) correlative CT, which demonstrates the partial cystic component (*arrow*). On surgery, the patient was found to have a cystic parathyroid adenoma in the superior mediastinum (of which the cystic component was only partially visualized on neck ultrasound).

thyromegaly.[15,17] Due to lack of an acoustic window, ultrasound also has limited sensitivity in detecting ectopic mediastinal parathyroid glands.

On sestamibi scan, parathyroid adenomas demonstrate early and intense uptake of sestamibi due to their increased mitochondrial activity, which may be obscured by similar level of tracer uptake in the thyroid gland. Approximately 60% of parathyroid adenomas demonstrate persistent tracer uptake, due to slower washout rate than the thyroid, and are detected as a focus of increased radiotracer on 2-hour delayed planar images[18] (**Figs. 6** and **7**). A second variant of parathyroid adenoma demonstrates early washout of tracer similar to the thyroid gland; these are harder to appreciate but can be detectable as a focal bulge in the contour of the thyroid gland on the immediate planar images. In addition, some adenomas demonstrate more intense uptake of tracer than the thyroid gland on early-phase images, which can aid in their detection. It is important to mention all focal abnormalities when reporting sestamibi scans and to correlate them with anatomic imaging of the thyroid gland. In some cases, there is persistent radiotracer uptake within the thyroid gland on delayed phase images, commonly seen in elderly individuals or in patients with diffuse thyroid disease; an even more delayed acquisition, such as a 4-hour delay, to allow for better clearance of the radiopharmaceutical from the thyroid gland, can be beneficial. SPECT images can be performed directly after the immediate planar images or at the 2-hour delay time point, and they increase sensitivity for detection of parathyroid adenomas due to 3-dimensional images that improve visualization of superimposed structures. Availability of CT images for localization can further increase sensitivity and diagnostic confidence in parathyroid adenomas and can facilitate comparison with other imaging studies and assist the surgeon in finding the adenoma. The diagnostic performance of scintigraphy with SPECT is generally comparable to ultrasound,

Box 1
Differential considerations

- Lymph node
- Exophytic thyroid nodule
- Lipoma/fat lobule
- Vascular structures
- Metastatic thyroid cancer
- Other cervical and mediastinal lesions

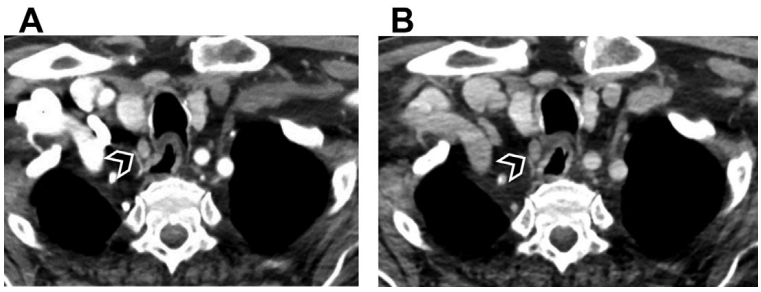

Fig. 9. Typical appearance of a parathyroid adenoma on 4DCT. Axial (*A*) arterial-phase image demonstrates an enhancing soft tissue nodule (*arrowheads*) in the tracheoesophageal groove with (*B*) venous-phase rapid washout, consistent with parathyroid adenoma. Patient underwent selective exploration of the right neck, and intraoperative parathyroid hormone levels dropped from 88 to 34 pg/mL.

with added benefit for detecting mediastinal adenomas (**Fig. 8**). In a recent meta-analysis, the sensitivity ranged between 57% and 100% with a pooled sensitivity of 84%.[16] In another meta-analysis of planar, SPECT, and SPECT/CT with Tc-99m sestamibi for detecting parathyroid adenomas, the pooled sensitivities were 63%, 66%, and 84%, and the PPVs were 90%, 82%, and 95%, respectively.[19] It is important to note that combining scintigraphy with ultrasound provides an incremental value in diagnostic accuracy of parathyroid adneomas.[4,15]

On 4DCT images, parathyroid adenomas are most conspicuous on arterial-phase images where they demonstrate avid enhancement, with rapid washout on venous-phase images (**Figs. 9** and **10**). The main concern with 4DCT is the radiation exposure; thus, it is reserved for cases in which

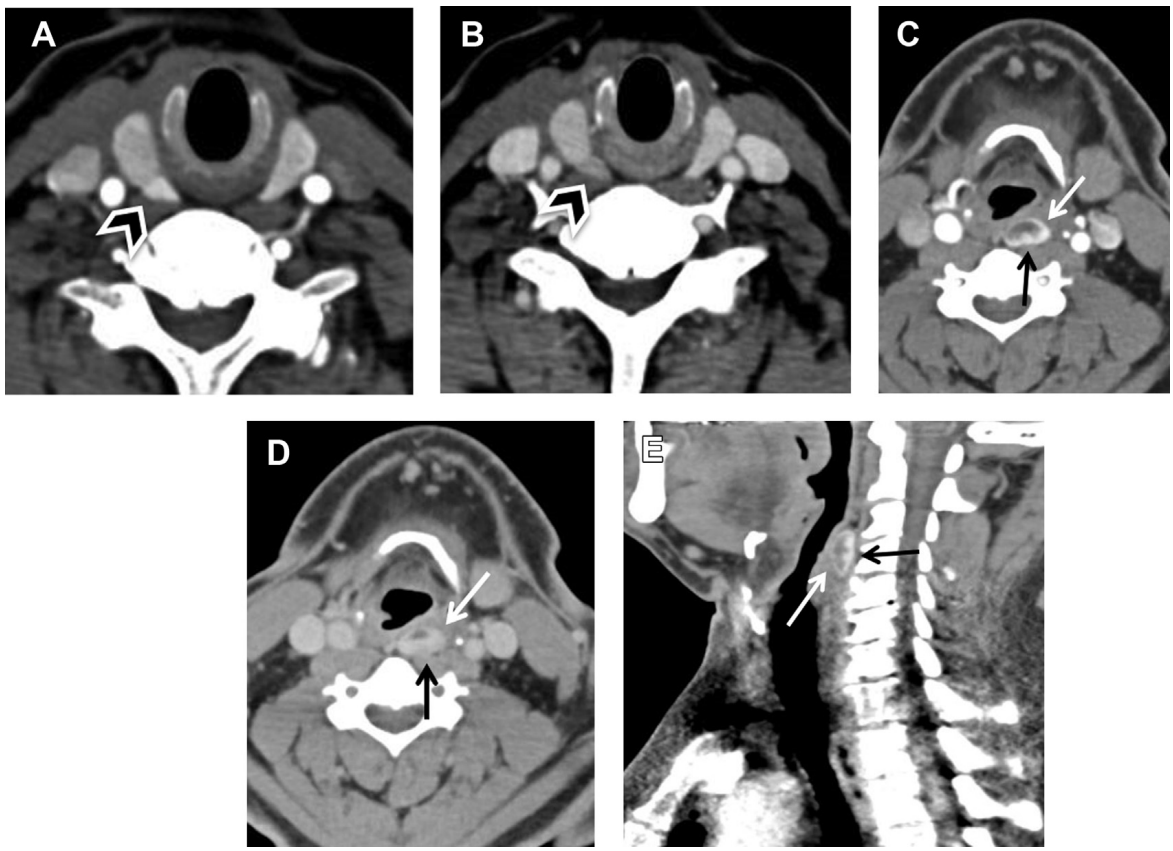

Fig. 10. Superior parathyroid adenoma on 4DCT. Typical appearance of a right superior parathyroid adenoma (*arrowheads*) seen on (*A*) arterial and (*B*) venous-phase images as a hyperenhancing soft tissue nodule directly posterior to the thyroid gland, with rapid washout. (*C*, *D*, *E*) Ectopic parathyroid adenoma (*arrows*) detected as a retropharyngeal nodule just anterior to the cervical spine, demonstrating peripheral (*C*) arterial hyperenhancement, with peripheral washout but central filling on the (*D*) venous phase, suspicious for parathyroid adenoma. This adenoma was causing mass effect on the posterior wall of the hypopharynx on sagittal reconstruction (*E*).

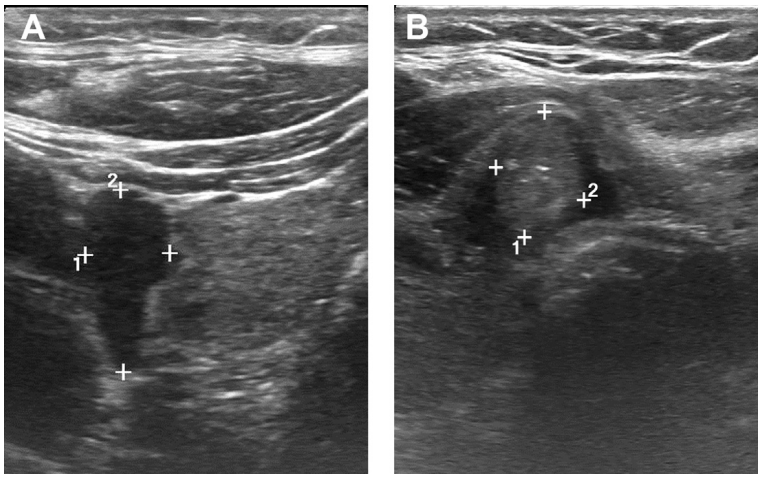

Fig. 11. Parathyroid adenoma and incidental papillary thyroid cancer. (*A*) Transverse grayscale image shows a parathyroid adenoma (*cursors*) adjacent to the right lobe of the thyroid. (*B*) Transverse view of the isthmus shows a solid, isoechoic, taller-than-wide nodule (*cursors*) with punctate echogenic foci. This TR5 nodule by American College of Radiology Thyroid Imaging, Reporting and Data System criteria measured 1.1 cm and was histologically confirmed to be a papillary thyroid cancer.

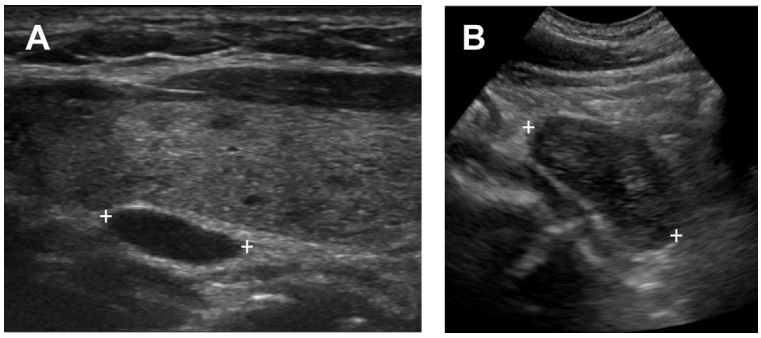

Fig. 12. Multigland adenomas. (*A*) Longitudinal grayscale view of the right neck shows superior parathyroid adenoma (*cursors*) posterior to the right thyroid. (*B*) An additional view of the low right neck obtained with a transvaginal probe shows a second parathyroid adenoma (*cursors*) of the inferior gland.

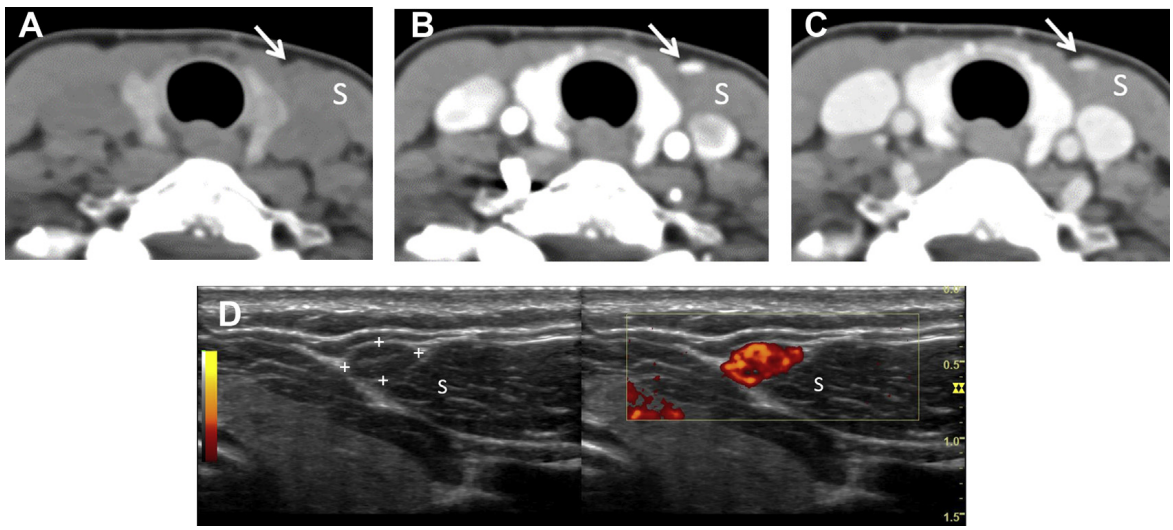

Fig. 13. Reimplanted parathyroid. A 56-year-old woman status post parathyroidectomy with reimplantation of one gland presents with recurrent hyperparathyroidism. (*A–C*) 4DCT images demonstrate a small nodule (*arrows*) anterior to the sternocleidomastoid muscle (S) that enhances avidly in the (*B*) arterial phase and washes out in the (*C*) venous phase, typical of a parathyroid adenoma. (*D*) Preoperative ultrasound was performed for marking the reimplanted gland, and demonstrates an enlarged parathyroid gland (*cursors*) superficial to the most medial aspect of the left sternocleidomastoid muscle (S) with intense hypervascularity.

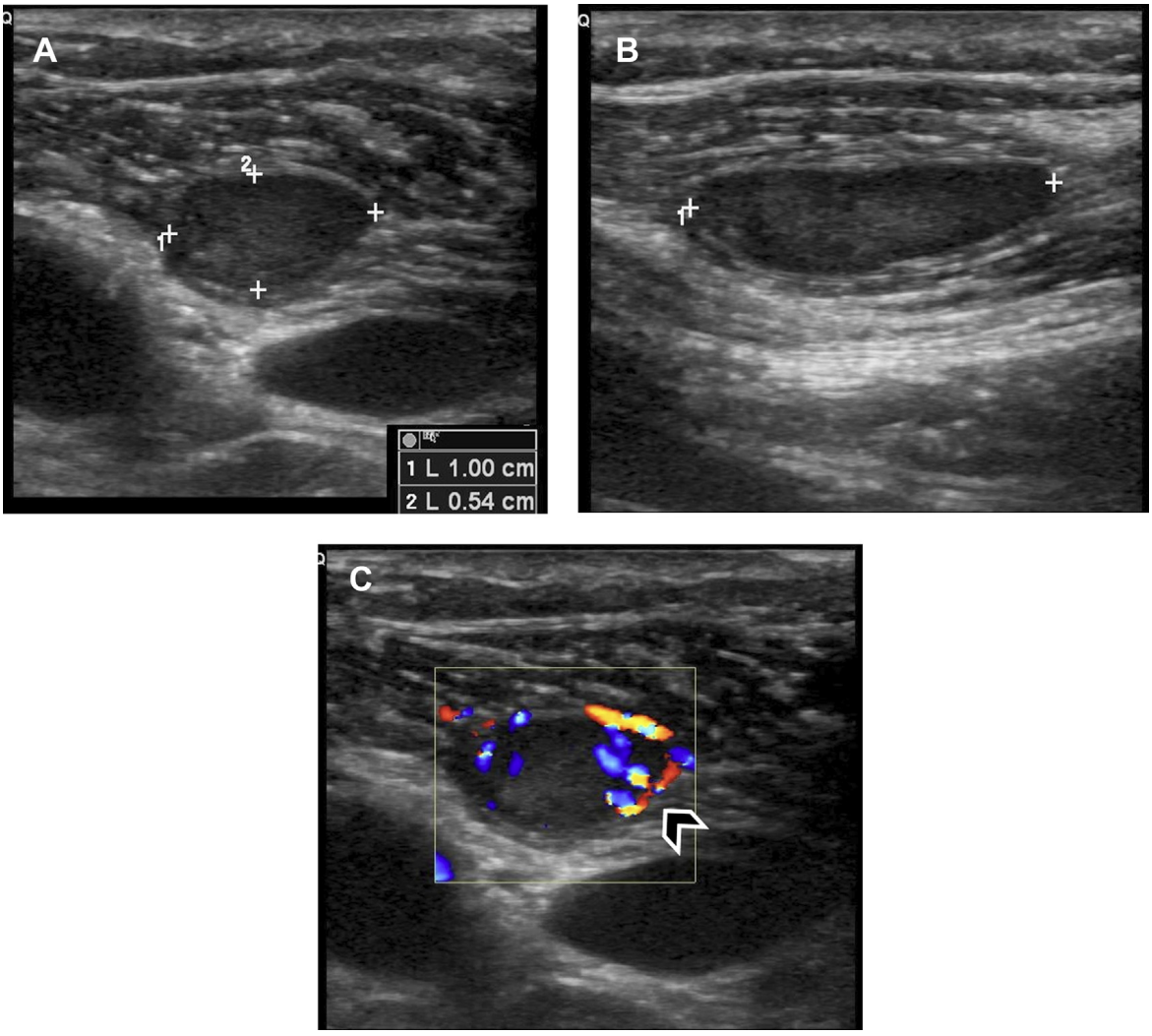

Fig. 14. Ectopic parathyroid adenoma. (*A*) Axial and (*B*) sagittal B-mode and (*C*) axial color Doppler images in a 45-year-old man with prior history of papillary thyroid cancer status post thyroidectomy and parathyroidectomy 19 years ago, with parathyroid reimplantation in the left forearm presents with persistent elevated calcium and elevated parathyroid hormone level of 120 pg/mL (reference range 14–64). Neck ultrasound images demonstrate a hypoechoic nodule (*cursors* in *A* and *B*) along the cervical lymph node chain at level 3 overlying the great vessels with internal vascularity (*arrowhead* in *C*) and a prominent feeding vessel. The radiologic differential considerations were recurrent metastatic lymph node versus ectopic parathyroid adenoma. Thyroglobulin levels in the serum and in the nodule aspirate were undetectable (<0.1 ng/mL). Cytology and surgical pathology were consistent with parathyroid adenoma.

ultrasound and sestamibi were nonlocalizing or discordant, or for patients with persistent or recurrent hyperparathyroidism after neck exploration.[20,21] In addition, 4DCT demonstrates higher sensitivity for detecting multigland disease.[21] Compared with ultrasound and SPECT, a 4DCT might provide a similar to slightly improved performance with sensitivity of 73.0% to 89.4%.[15,17] A cost-utility analysis in 2011 demonstrated that surgeons use ultrasound and scintigraphy as first-line modalities for localization and reserve 4DCT for more challenging or reoperative cases.[1]

Differential Diagnosis

A variety of cervical and superior mediastinal structures can be mistaken for a parathyroid adenoma (**Box 1**). On ultrasound, differential considerations for parathyroid adenomas include well-defined cervical nodules, such as lymph nodes, which are typically differentiated by their location along lymph node chains and an echogenic fatty hilum with hilar vascularity. Consequentially, morphologically abnormal lymph nodes with loss of the fatty hilum or peripheral vascularity can be harder to differentiate from parathyroid adenomas

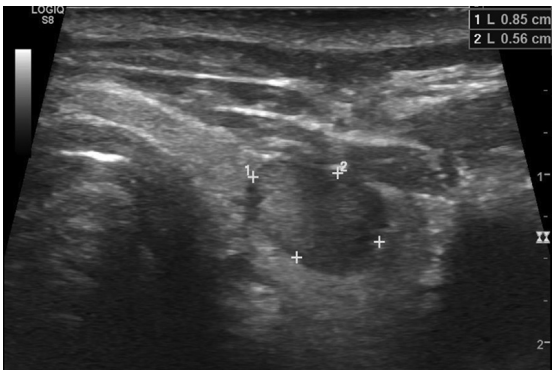

Fig. 15. Intrathyroid parathyroid adenoma. Transverse sonogram of the left thyroid shows a solid, hypoechoic intrathyroidal nodule (*cursors*). FNA showed a PTH tissue washout level of 8832 pg/mL, consistent with an intrathyroidal parathyroid adenoma.

than morphologically benign nodes. If the nodule is located lateral to the common carotid artery, it is very unlikely to be a parathyroid adenoma. Other differential considerations include exophytic thyroid nodules or separate thyroid lobulations in which a prominent thin hyperechoic septum is seen between 2 portions of the thyroid gland. This is most often along the posterior border of the mid to lower portion of the thyroid and is due to an anatomic variant known as the tubercle of Zuckerkandl. This can be differentiated on ultrasound by examining the entire margins of the nodule; a prominent lobulation or exophytic nodule typically has a thin portion that is still communicating with the thyroid gland. An anechoic fluid-filled esophageal diverticulum or a vascular structure might be mistaken for a very hypoechoic parathyroid adenoma; in these scenarios, color Doppler and varying manual pressure with the transducer can aid in the diagnosis.

On sestamibi scan, a thyroid adenoma can be differentiated from a parathyroid adenoma with a dual tracer study in which a thyroid adenoma demonstrates uptake of Tc-99m pertechnetate or I-123 but a parathyroid adenoma remains photopenic (cold). Alternatively, correlation with ultrasound

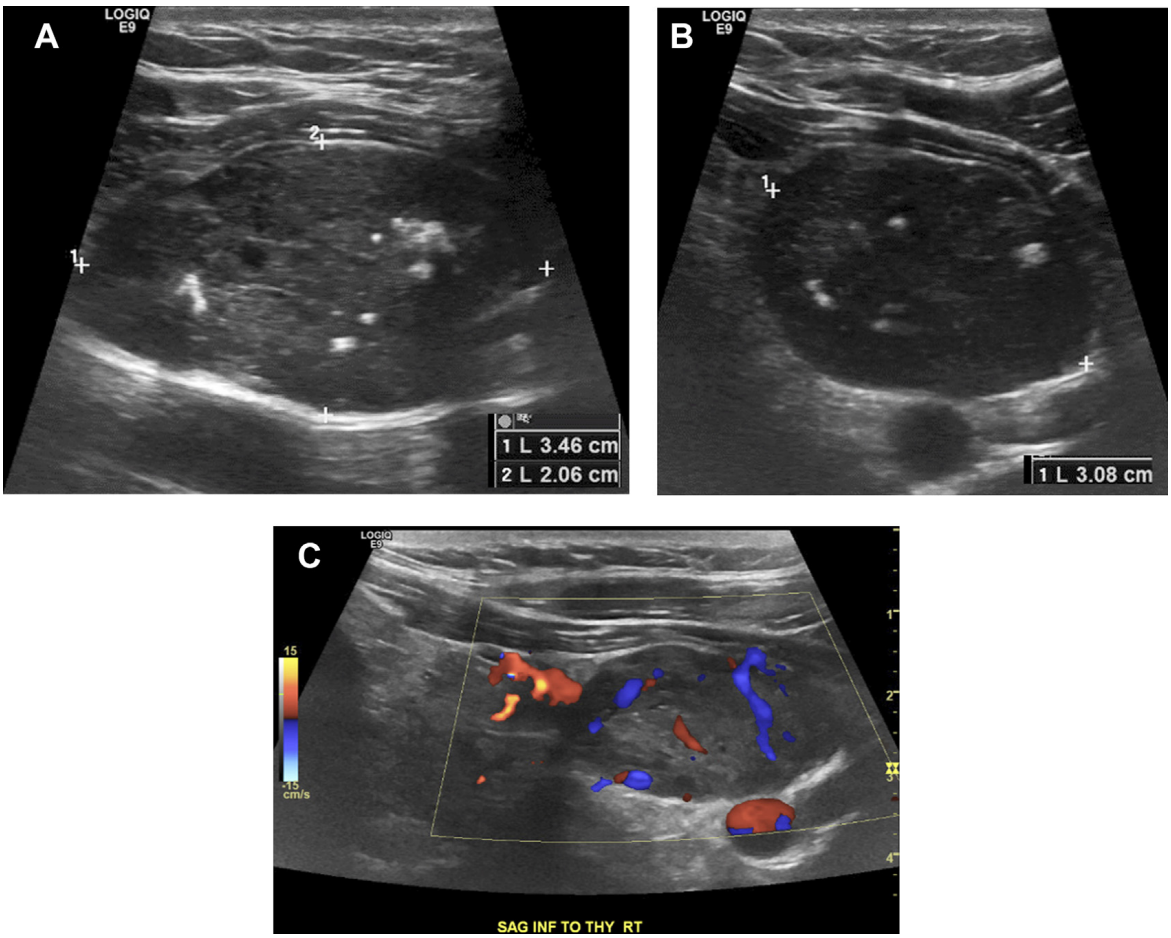

Fig. 16. Parathyroid carcinoma. (*A*) Sagittal and (*B*) axial B-mode images and (*C*) axial color Doppler images in a 38-year-old man with primary hyperparathyroidism demonstrate an enlarged parathyroid with internal calcifications (*cursors* in *A* and *B*). Pathology was consistent with parathyroid carcinoma with negative surgical margins.

can establish the diagnosis of a thyroid rather than a parathyroid nodule. Other causes of false positive sestamibi uptake in the neck are rare and include malignancies such as lung, breast, and papillary thyroid cancer, in addition to reactive and metastatic lymph nodes.[11]

On 4DCT, causes of false positive findings include arterial hyperenhancing lesions, such as vascular structures, neuroendocrine tumors, and pathologic lymph nodes such as those metastatic from hypervascular primary malignancies, namely papillary thyroid cancer. It is important to perform noncontrast CT as part of the 4DCT protocol to differentiate hyperenhancement from hyperdense lesions such as ectopic thyroid nodules and mildly calcified lymph nodes.

Pearls, Pitfalls, and Variants

A major advantage of parathyroid sonography is its ability to evaluate thyroid nodules. Because these patients are typically going to the operating room to resect an abnormal parathyroid gland, it is also important to know whether there is a thyroid nodule that needs attention. Any suspicious thyroid nodule should either undergo fine needle aspiration (FNA) before surgery or should be resected during the parathyroid operation (**Fig. 11**). Parathyroid adenomas are most often solitary, but approximately 5% to 10% of patients will have involvement of 2 glands. It is important not to fall for the "happy eye syndrome" once a single adenoma is identified (**Fig. 12**). In addition, 4-gland hyperplasia can be seen in the subset of patients with secondary or tertiary hyperparathyroidism who are referred for surgical resection in cases of severe osteopenia, uncontrolled symptoms, calciphylaxis, or very high parathyroid hormone levels; preoperative imaging is not routinely performed in these patients, but it can be useful to identify ectopic gland location or asymmetric gland hyperplasia.[22] In these patients, a portion of a gland can be reimplanted in the forearm, or anterior to abdominal wall musculature or sternocleidomastoid muscle (**Fig. 13**).

Lymph nodes are typically differentiated from parathyroid adenomas by their location and their morphologic features, but ectopic parathyroid adenomas may present in the expected location of cervical lymph nodes, rendering their diagnosis more challenging (**Fig. 14**). In these cases, additional passes can be performed during the FNA for determining PTH levels in the nodule.

Another diagnostic challenge arises with intrathyroid parathyroid adenomas (**Fig. 15**), especially in patients with a multinodular thyroid gland. Determining PTH levels in the nodule is also crucial in these cases because it is harder to differentiate a parathyroid adenoma from a thyroid nodule on cytology than it is to differentiate a parathyroid adenoma from a lymph node.

List: Pearls and Pitfalls

- Look for a fatty hilum to differentiate lymph nodes from adenomas
- Given that intrathyroidal parathyroid adenomas are rare, if you suspect one, then consider sampling for PTH levels before surgery
- Always look for multigland disease

List: Variants

- Ectopic locations of parathyroid adenomas
- Internal cystic spaces in cystic adenomas
- Focal hyperechoic areas or internal heterogeneity

WHAT THE REFERRING PHYSICIAN NEEDS TO KNOW

Bilateral neck exploration has been the classic surgical approach for parathyroidectomy; however, with preoperative localization imaging studies, a minimally invasive technique is possible in a large subset of patients, providing improved cosmesis, shorter operation time, shorter hospital stay, lower cost of care, lower morbidity, and high cure rates.[1] For the surgeon, when localization with ultrasound and sestamibi is concordant, a minimally invasive technique can be performed, with intraoperative confirmation of normalized PTH levels. The information relayed to the referring provider should include the accurate size and location of the parathyroid adenoma, as well as presence of any features concerning for carcinoma, such as unusually large size, invasion of the adjacent vessels or of the thyroid capsule, irregular margins, or calcifications (**Fig. 16**).

It is obvious that the presence of multiple enlarged glands should be conveyed, as it might alter the surgical approach. If a suspected parathyroid nodule has atypical sonographic features, FNA can be performed to confirm the diagnosis, especially if scintigraphy was discordant. In patients with challenging surgery, such as those with prior neck radiation or multiple prior neck surgeries, microwave or alcohol ablation of parathyroid adenomas can be offered as a therapeutic procedure.[23–25]

List: What the Referring Physician Needs to Know

- Location of parathyroid adenoma: side, inferior, superior, ectopic
- Multiplicity of adenomas
- Presence of any features concerning for carcinoma
- Need for PTH sampling for confirmation of atypical or intrathyroid nodule
- Amenability to alcohol ablation, especially in poor surgical candidates

SUMMARY

Imaging plays an important role in management of PHPT, particularly in localizing parathyroid adenomas and helping select patients who are eligible for minimally invasive surgery. Ultrasound and sestamibi scan remain the first line of imaging, with 4DCT reserved for more challenging cases.

REFERENCE

1. Mallick R, Chen H. Diagnosis and management of hyperparathyroidism. Adv Surg 2018;52(1):137–53.
2. Yeh MW, Ituarte PH, Zhou HC, et al. Incidence and prevalence of primary hyperparathyroidism in a racially mixed population. J Clin Endocrinol Metab 2013;98(3):1122–9.
3. Macfarlane DP, Yu N, Leese GP. Subclinical and asymptomatic parathyroid disease: implications of emerging data. Lancet Diabetes Endocrinol 2013;1(4):329–40.
4. Walker MD, Silverberg SJ. Primary hyperparathyroidism. Nat Rev Endocrinol 2018;14(2):115–25.
5. Silverberg SJ, Clarke BL, Peacock M, et al. Current issues in the presentation of asymptomatic primary hyperparathyroidism: proceedings of the Fourth International Workshop. J Clin Endocrinol Metab 2014;99(10):3580–94.
6. Corbetta S. Normocalcemic hyperparathyroidism. Front Horm Res 2019;51:23–39.
7. Taslakian B, Trerotola SO, Sacks B, et al. The essentials of parathyroid hormone venous sampling. Cardiovasc Intervent Radiol 2017;40(1):9–21.
8. Gilmour JR. The gross anatomy of the parathyroid glands. J Pathol Bacteriol 1938;46(1):133–49.
9. Policeni BA, Smoker WR, Reede DL. Anatomy and embryology of the thyroid and parathyroid glands. Semin Ultrasound CT MR 2012;33(2):104–14.
10. Lyden ML, Wang TS, Sosa JA. Surgical anatomy of parathyroid glands. In: Carty SE, Chen W, editors. Uptodate; 2019. Available at: https://www.uptodate.com/contents/surgical-anatomy-of-the-parathyroid-glands.
11. Vaz A, Griffiths M. Parathyroid imaging and localization using SPECT/CT: initial results. J Nucl Med Technol 2011;39(3):195–200.
12. Mellnick VM, Middleton WD. Parathyroid sonography. Ultrasound Clin 2014;9(3):339–49.
13. Devcic Z, Jeffrey RB, Kamaya A, et al. The elusive parathyroid adenoma: techniques for detection. Ultrasound Q 2013;29(3):179–87.
14. Kamaya A, Quon A, Jeffrey RB. Sonography of the abnormal parathyroid gland. Ultrasound Q 2006;22(4):253–62.
15. Treglia G, Trimboli P, Huellner M, et al. Imaging in primary hyperparathyroidism: focus on the evidence-based diagnostic performance of different methods. Minerva Endocrinol 2018;43(2):133–43.
16. Nafisi Moghadam R, Amlelshahbaz AP, Namiranian N, et al. Comparative diagnostic performance of ultrasonography and 99mtc-sestamibi scintigraphy for parathyroid adenoma in primary hyperparathyroidism; systematic review and meta- analysis. Asian Pac J Cancer Prev 2017;18(12):3195–200.
17. Cheung K, Wang TS, Farrokhyar F, et al. A meta-analysis of preoperative localization techniques for patients with primary hyperparathyroidism. Ann Surg Oncol 2012;19(2):577–83.
18. Eslamy HK, Ziessman HA. Parathyroid scintigraphy in patients with primary hyperparathyroidism: 99mTc sestamibi SPECT and SPECT/CT. Radiographics 2008;28(5):1461–76.
19. Wei WJ, Shen CT, Song HJ, et al. Comparison of SPET/CT, SPET and planar imaging using 99mTc-MIBI as independent techniques to support minimally invasive parathyroidectomy in primary hyperparathyroidism: a meta-analysis. Hell J Nucl Med 2015;18(2):127–35.
20. Machado NN, Wilhelm SM. Diagnosis and evaluation of primary hyperparathyroidism. Surg Clin North Am 2019;99(4):649–66.
21. Tian Y, Tanny ST, Einsiedel P, et al. Four-dimensional computed tomography: clinical impact for patients with primary hyperparathyroidism. Ann Surg Oncol 2018;25(1):117–21.
22. Pitt SC, Sippel RS, Chen H. Secondary and tertiary hyperparathyroidism, state of the art surgical management. Surg Clin North Am 2009;89(5):1227–39.
23. Singh Ospina N, Thompson GB, Lee RA, et al. Safety and efficacy of percutaneous parathyroid ethanol ablation in patients with recurrent primary hyperparathyroidism and multiple endocrine neoplasia type 1. J Clin Endocrinol Metab 2015;100(1):E87–90.
24. Kitaoka M. Ultrasonographic diagnosis of parathyroid glands and percutaneous ethanol injection therapy. Nephrol Dial Transplant 2003;18(Suppl 3):ii27–30.
25. Liu F, Yu X, Liu Z, et al. Comparison of ultrasound-guided percutaneous microwave ablation and parathyroidectomy for primary hyperparathyroidism. Int J Hyperthermia 2019;36(1):835–40.